



Contents lists available at [SciVerse ScienceDirect](http://SciVerse.ScienceDirect.com)

## Behavioural Brain Research

journal homepage: [www.elsevier.com/locate/bbr](http://www.elsevier.com/locate/bbr)



### Research report

# The salience network contributes to an individual's fluid reasoning capacity

Zhina Yuan<sup>a</sup>, Wen Qin<sup>a</sup>, Dawei Wang<sup>a</sup>, Tianzi Jiang<sup>b</sup>, Yunting Zhang<sup>a,\*</sup>, Chunshui Yu<sup>a,c,\*\*</sup>

<sup>a</sup> Department of Radiology, Tianjin Medical University General Hospital, Tianjin, China

<sup>b</sup> LIAMA Center for Computational Medicine, National Laboratory of Pattern Recognition, Institute of Automation, Chinese Academy of Sciences, Beijing, China

<sup>c</sup> School of Medical Imaging, Tianjin Medical University, Tianjin, China

### ARTICLE INFO

#### Article history:

Received 18 October 2011  
Received in revised form 14 January 2012  
Accepted 17 January 2012  
Available online xxx

#### Keywords:

Fluid reasoning  
Raven's Progressive Matrices  
Gray matter volume  
Voxel-based morphometry  
Regional homogeneity  
Magnetic resonance imaging

### ABSTRACT

Fluid reasoning is the ability to think flexibly and logically, analyze novel problems and identify the relationships that underpin these problems independent of acquired knowledge. Although many functional imaging studies have investigated brain activation during fluid reasoning tasks, the neural correlates of fluid reasoning remain elusive. In the present study, we aimed to uncover the neural correlates of fluid reasoning by analyzing correlations between Raven's Standard Progressive Matrices (RSPM), an effective measure of fluid reasoning, and measures of regional gray matter volume (GMV) and regional homogeneity (ReHo) in a voxel-wise manner throughout the whole brain in 297 healthy young adults. The most important finding was that RSPM scores were positively correlated with both GMV and ReHo values in brain areas that belong to the salience network, including the dorsal anterior cingulate cortex and the fronto-insular cortex. Additionally, we found positive or negative correlations between RSPM scores and GMV or ReHo values in brain areas of the central-executive, default-mode, sensorimotor and visual networks. Our findings suggest that fluid reasoning ability is related to a variety of brain areas and emphasize the important contribution of the salience network to this ability.

© 2012 Elsevier B.V. All rights reserved.

### 1. Introduction

In cognitive psychology, fluid reasoning refers to the capacity of relational reasoning that is used to identify relationships, comprehend implications and draw inferences in a novel context. Empirically, it is not only considered as a higher cognitive factor that is central to general intelligence [1] but also is strongly associated with working memory and *g* factor [2]. Fluid reasoning capacity influences how fast and how much a person learns and affects their ability to manage and manipulate information

during the reasoning process [3]. A widely used neuropsychological test, Raven's Progressive Matrices (RPM), is broadly accepted as a culture-free, nonverbal measure of an individual's capacity of fluid reasoning [4]. The capacity of fluid reasoning is thought to be responsible for an individual's performance in a broad variety of cognitive tasks.

The neural substrates of fluid reasoning have been extensively investigated by functional imaging studies using healthy participants who performed a variety of reasoning tasks [5–12]. Using the RPM or its derivatives as experimental tasks, several functional magnetic resonance imaging (fMRI) and positron emission tomography (PET) studies showed activation in the medial and lateral prefrontal and posterior parietal cortices during the fluid reasoning process [1–3,5,6,9,10,13]. Although these task-based functional imaging studies can identify brain regions engaged in the reasoning process, they cannot identify the neural correlates of the capacity of fluid reasoning because while functional imaging measures active processing, capacity itself is not a process but rather a constraint on processing. To identify the neural correlates of the capacity of fluid reasoning, a few task-based fMRI studies investigated correlations between the magnitude of brain activation and individual RPM scores and found significant correlations in the lateral prefrontal and parietal cortices [1,14,15].

In addition to task-based functional imaging studies, other imaging techniques have been applied to study the neural correlates of the capacity of fluid reasoning. Most of these studies were designed to investigate general intelligence as assessed by

*Abbreviations:* ACC, anterior cingulate cortex; AI, anterior insula; BOLD, blood oxygenation level-dependent; CEN, central executive network; dACC, dorsal anterior cingulate cortex; DARTEL, diffeomorphic anatomical registration through exponentiated Lie algebra; DMN, default-mode network; FIC, fronto-insular cortex; FG, fusiform gyrus; FWHM, full width at half maximum; GM, gray matter; GMV, gray matter volume; IQ, intelligence quotient; KCC, Kendall's coefficient of concordance; MNI, Montreal Neurological Institute; OFC, orbitofrontal cortex; PCC/Pcu, posterior cingulate cortex/precuneus; PHG, parahippocampal gyrus; ReHo, regional homogeneity; RPM, Raven's Progressive Matrices; RSPM, Raven's Standard Progressive Matrices; VBM, voxel-based morphometry.

\* Corresponding author at: Department of Radiology, Tianjin Medical University General Hospital, No. 154, Anshan Road, Heping District, Tianjin 300052, China.

\*\* Corresponding author at: Department of Radiology, Tianjin Medical University General Hospital, No. 154, Anshan Road, Heping District, Tianjin 300052, China. Tel.: +86 22 60362990; fax: +86 22 60362990.

E-mail addresses: [cjr.zhangyunting@vip.163.com](mailto:cjr.zhangyunting@vip.163.com) (Y. Zhang), [chunshuiyu@yahoo.cn](mailto:chunshuiyu@yahoo.cn) (C. Yu).

the intelligence quotient (IQ) score, an integrated reflection of crystal and fluid intelligence [16]. Structural MRI studies found that regional gray (GMV) and white matter volumes of widely distributed brain areas were correlated with IQ in healthy individuals [17–21]. Diffusion MRI showed that the integrity of some white matter fiber tracts and the efficiency of brain structural organization are associated with general intelligence [22–24]. Resting-state fMRI revealed that an individual's IQ score can be predicted by Regional Homogeneity (ReHo), functional connectivity and functional network efficiency [25–27]. However, these studies cannot exclusively reflect the neural substrate of fluid reasoning because only the fluid intelligence component of IQ reflects the capacity of fluid reasoning. With regard to the neural correlates of fluid reasoning in healthy adults, only one study has investigated correlations between GMV and fluid intelligence. The results emphasized the importance of the medial prefrontal cortex in fluid intelligence [28], although several studies on different patient populations have detected correlations between alterations in GMV and cognitive deficits as measured by RPM [29,30].

Taken together, there is lack of comprehensive studies that used a large sample of healthy subjects to investigate the neural correlates of the capacity of fluid reasoning. In the present study, we aimed to address the question by analyzing correlations between RPM scores and regional GMV and ReHo in a voxel-wise manner throughout the whole brain in a large sample of 297 healthy young adults. The combination of structural and resting-state functional MRI data may improve our understanding of the neural correlates of individual differences in fluid reasoning.

## 2. Materials and methods

### 2.1. Participants

A total of 324 right-handed, healthy, young adults were recruited via advertisements. The participants had not suffered from any psychiatric or neurological disorders and did not have any contraindications to MRI scan. Conventional brain MRI scans were performed on all subjects, and these did not reveal any visible lesions. Among the participant pool, 16 participants were excluded due to a lack of behavioral data, 2 participants were excluded due to poor image quality and 9 participants were excluded due to extremely low scores on the Chinese RSPM norm (for details see Table S1–S3 in Supplementary Materials). Therefore, for VBM analyses, 297 healthy participants (156 females, 141 males) were included in the study. For ReHo analysis, 13 participants were excluded due to excessive head motions, resulting in 284 participants (152 females, 132 males). All subjects signed a written, informed consent form that was approved by the Medical Research Ethics Committee of Tianjin Medical University.

### 2.2. Behavioral examination

The RPM is designed to test the ability to reason and solve new problems without relying extensively on declarative knowledge derived from schooling or previous experience [31]. As stated by Snow et al. [4], the RPM test is often regarded as an ideal measure of fluid reasoning that requires verbal, spatial and mathematical problem-solving abilities [4]. Matrix tests are composed of a series of nonverbal pictures that are visually incomplete and the response must be chosen from an array of possible answers. In this study, we chose to use Raven's Standard Progressive Matrices (RSPM) [32] as a test for the capacity of fluid reasoning. The RSPM consists of 60 matrix-reasoning problems, with increasing complexity and difficulty, in which participants must identify relevant visual features based on the spatial organization of an array of visual stimuli and then select one of several possible answers that matches these identified features. In our examination, all participants were told to study each problem until they had determined the best answer, with no explicit time limit. The RSPM score of each subject is the number of correct items out of 60 possible items, but it is not a scaled score.

### 2.3. MR data acquisition

MR images were acquired by a 3.0T MR scanner (Signa Excite HDx; GE Healthcare, Milwaukee, WI). Tight but comfortable foam padding was used to minimize head motion, and earplugs were used to reduce scanner noise. Resting-state fMRI scans were performed by an echo planar imaging (EPI) sequence with scan

parameters of repetition time (TR)=2000 ms, echo time (TE)=30 ms, flip angle (FA)=90°, matrix=64 × 64, field of view (FOV)=240 mm × 240 mm, slice thickness=4 mm without gap. Each brain volume comprised 40 axial slices, and each functional run contained 180 volumes. During fMRI scans, all subjects were instructed to keep their eyes closed, to stay as motionless as possible, to think of nothing in particular and not to fall asleep. Finally, a high-resolution T1-weighted brain volume (BRAVO) 3D MRI sequence with 176 contiguous sagittal slices was performed with the following scan parameters: TR=8.1 ms, TE=3.1 ms, inversion time=450 ms, FOV=256 mm × 256 mm, slice thickness=1.0 mm without gap, FA=13°, matrix=256 × 256. The resting-state fMRI data took 6 min and 10 s to acquire for each subject.

### 2.4. Data analysis

#### 2.4.1. VBM analysis

The VBM analysis was performed using Statistical Parametric Mapping (SPM8; <http://www.fil.ion.ucl.ac.uk/spm/software/spm8>). The structural MR images were segmented into gray matter (GM), white matter and cerebrospinal fluid using the standard unified segmentation model in SPM8. Following segmentation, GM population templates were generated from the entire image dataset using diffeomorphic anatomical registration through the exponentiated Lie algebra (DARTEL) technique [33]. After an initial affine registration of the GM DARTEL template to the tissue probability map in Montreal Neurological Institute (MNI) space (<http://www.mni.mcgill.ca/>), non-linear warping of GM images was performed to the DARTEL GM template in MNI space with a resolution of 1.5 mm<sup>3</sup> (as recommended for the DARTEL procedure). The GMV of each voxel was obtained by multiplying the GM concentration map by the non-linear determinants derived from the spatial normalization step. Finally, to compensate for residual between-subject anatomical differences, the GMV images were smoothed with a FWHM kernel of 8 mm. In effect, the analysis of modulated data tests for regional differences in the absolute volume of brain and removes the confounding effect of variance in individual brain sizes. After spatial pre-processing, the smoothed, modulated, normalized GMV maps were used for statistical analysis.

Voxel-based partial correlation analyses were carried out to test correlations between GMVs and RSPM scores. Age and gender were entered as covariates of no interest. Correction for multiple comparisons was performed using Monte Carlo simulation. A corrected threshold of  $P < 0.01$  (two-tailed) was derived from a combined threshold of  $P < 0.01$  for each voxel, and a cluster size of >628 voxels was determined using the AlphaSim program in AFNI software (Parameters: single voxel  $P = 0.01$ , 5000 simulations, FWHM = 8 mm, cluster connection radius = 2.5 mm with gray matter mask, <http://afni.nimh.nih.gov/>).

#### 2.4.2. ReHo analysis

Preprocessing and statistical analysis of the resting-state fMRI data were conducted using SPM8 (<http://www.fil.ion.ucl.ac.uk/spm/software/spm8>). The first 10 volumes of each functional time series were discarded to allow the longitudinal magnetization to reach a steady state and to allow participants acclimate to the scanning environment. The 170 remaining images were corrected for acquisition time delay between different slices and realigned to the first volume. Head motion parameters were computed by estimating translation in each direction and angular rotation on each axis for each volume, which provided a record of head position. We controlled for head motion using a threshold of 2.0 mm translation in any cardinal direction and 2.0° rotation in each of the orthogonal x, y and z axes. After applying these parameters, only 284 subjects satisfied the requirements for inclusion. The realigned functional volumes were then spatially normalized to the MNI space using the normalization parameters estimated by T1 structural image unified segmentation, re-sampled to 2-mm<sup>3</sup> voxel and smoothed with a Gaussian kernel of 4 mm full width at half maximum (FWHM). Several sources of spurious variance, including estimated motion parameters, linear drift, and average BOLD signals in ventricular and white matter regions, were removed from the data through linear regression. After the removal of variance, a temporal filtration (0.01–0.08 Hz) was performed to reduce the effect of low-frequency drifts and high-frequency noise.

Kendall's coefficient of concordance (KCC) was used to measure the correlation of the time series of a given voxel with the time series of its 26 nearest neighbors. Individual ReHo maps were generated by calculating KCC within a gray matter mask in a voxel-wise manner using REST software (<http://restfmri.net/forum/index.php>). When the center cube was on the edge of the gray matter mask, we only calculated ReHo for a voxel if all of remaining nearest voxels were within the gray matter mask. For each subject, KCC maps were normalized by dividing KCC in each voxel by the mean KCC of total gray matter [34].

Voxel-based partial correlation analyses were performed to test correlations between ReHo values and RSPM scores. Age and gender were entered as covariates of no interest. Correction for multiple comparisons was performed using Monte Carlo simulation. A corrected threshold of  $P < 0.01$  (two-tailed) was derived from a combined threshold of  $P < 0.01$  for each voxel and a cluster size of >71 voxels was determined using the AlphaSim program in AFNI software (Parameters: single voxel  $P = 0.01$ , 5000 simulations, FWHM = 4 mm, cluster connection radius = 3.3 mm, with gray matter mask, <http://afni.nimh.nih.gov/>).

**Table 1**

Demographic and behavioral data. A total of 297 subjects were included in the voxel-based morphometry (VBM) analysis. From that sample, 284 subjects were included in the regional homogeneity (ReHo) analysis.

Items	Total subjects
<b>VBM analysis</b>	
No. of subjects	297
Males/females	141/156
Age (years)	22.7 ± 2.5(18–29)
RSPM score	53.5 ± 5.5(34–60)
<b>ReHo analysis</b>	
No. of subjects	284
Males/females	132/152
Age (years)	22.8 ± 2.4(18–29)
RSPM score	53.6 ± 5.5(34–60)

Abbreviations: ReHo, regional homogeneity; RSPM, Raven's Standard Progressive Matrices; VBM, voxel-based morphometry.

### 3. Results

#### 3.1. Demographic and behavioral data

The demographic and behavioral data are shown in Table 1. A total of 297 healthy participants (156 females, 141 males) were included in the VBM analysis, whereas 284 subjects (152 females, 132 males) were included in the ReHo analysis. The RSPM scores for all subjects ranged from 34 to 60. There were no significant gender differences ( $P > 0.05$ ) in RSPM scores and no significant correlation between age and RSPM score in subjects for either the VBM analysis or the ReHo analysis.

#### 3.2. Correlation between GMV and RSPM score

After correcting for multiple comparisons, RSPM scores were positively correlated with GMVs in the right fronto-insular cortex (FIC), the left anterior cingulate cortex (ACC) of the salience network, the bilateral temporal poles, the orbitofrontal cortices (OFC), the occipital lobes, and the left parahippocampal (PHG) and fusiform gyri (FG) (Table 2 and Fig. 1). There was no brain area whose GMV was negatively correlated with RSPM scores.

#### 3.3. Correlation between ReHo and RSPM score

Under the same thresholds used in the VBM analysis, RSPM scores were positively correlated with ReHo values in the right FIC of the salience network, the right middle frontal gyrus and temporal pole, and the left fusiform (FG) and parahippocampal gyri (PHG) (Table 3 and Fig. 2). In contrast, RSPM scores were negatively correlated with ReHo values in the bilateral sensorimotor cortex, the posterior cingulate cortex, the precuneus and the right inferior parietal lobule of the default-mode network (DMN) (Table 3 and Fig. 2).

**Table 2**

Brain areas whose gray matter volumes show significant correlations with RSPM scores.

Brain regions	Brodman areas	Cluster size (voxels)	Peak <i>t</i> values	Peak coordination in MNI ( <i>x, y, z</i> )
Right FIC	13/47	8712	5.02*	–14, 39, 21
Right temporal pole	38			
Left ACC	32			
Bilaeral OFC	10/11/25			
Left PHG, FG	20/35/36	1041	4.79	–24, –30, –23
Bilateral occipital lobes	17/18	1960	4.45	30, –93, –6
Left sensorimotor cortex	3/4/6	1385	3.96	–41, –20, 65
Right mid-cingulate cortex and medial parietal lobe	5/24/31	1626	3.50	5, –42, 59
Left temporal pole	38	710	3.47	–35, 0, –29

Abbreviations: ACC, anterior cingulate cortex; FIC, fronto-insular cortex; FG, fusiform gyrus; MNI, Montreal Neurological Institute; OFC, orbitofrontal cortex; PHG, parahippocampal gyrus; RSPM, Raven's Standard Progressive Matrices.

\*  $P < 0.01$ , corrected.

### 4. Discussion

The present study combined VBM analysis of structural MRI data and ReHo analysis of resting-state fMRI data to investigate the neural correlates of the capacity of fluid reasoning as measured by RSPM in a large sample of 297 healthy young adults. We found that RSPM scores were positively correlated with both GMV and ReHo in brain areas belonging to the salience network, including the dorsal ACC (dACC) and FIC, suggesting an important contribution of the salience network to the capacity of fluid reasoning.

The salience network mainly consists of the dACC and FIC and serves to identify the most relevant internal or extrapersonal stimuli to guide behavior [35]. Converging evidence suggests that the right FIC plays a critical and causal role in switching between the central executive network (CEN) and the DMN [36]. These networks are known to interact competitively during cognitive information processing [37,38]. The functional roles of nodes of the salience network have been hypothesized. The anterior insula (AI) is involved in the transient detection of salient stimuli and the initiation of attentional control signals that are sustained by the dACC and the ventrolateral and dorsolateral prefrontal cortices [39]. Specifically, the AI serves to identify salient stimuli from the vast and continuous stream of visual, auditory, tactile and other sensory inputs. Once a salient stimulus is detected, the AI initiates appropriate transient control signals to engage brain areas of the CEN that mediate attentional control, working memory and other higher order cognitive processes while disengaging the DMN via the von Economo neurons (VENs) [40] characterized by large axons which facilitate rapid relay of AI and dACC signals to other cortical regions [41]. Importantly, the switching mechanism helps to focus attention on external stimuli, and as a result, the identified stimulus takes on added significance or saliency [39]. Our finding that RSPM scores were positively correlated with both GMV and ReHo of brain areas of the salience network, especially the right FIC, suggests the importance of the development of the salience network for the capacity of fluid reasoning. This inference is supported by the following findings: (1) anatomically, several studies have revealed that gray matter volume and cortical thickness of brain areas of the salience network are positively correlated with IQ scores [28,42–44]; (2) functionally, fluid reasoning tasks are frequently reported to activate the FIC and dACC [1,2,6,10,15,45–47]; (3) the right uncinate fasciculus, an important white matter tract that is related to the salience network, has been reported to be related to individual intelligence [22]; (4) abnormalities in the salience network have been reported in frontotemporal dementia, characterized by deficits in social-emotional and executive functions [48,49]. Additionally, the cerebellar lobule VI is also a node of the salience network [50] and is involved in response correctness during a RPM-like task [3], which may explain the correlation we found between the ReHo of this structure and RSPM scores.

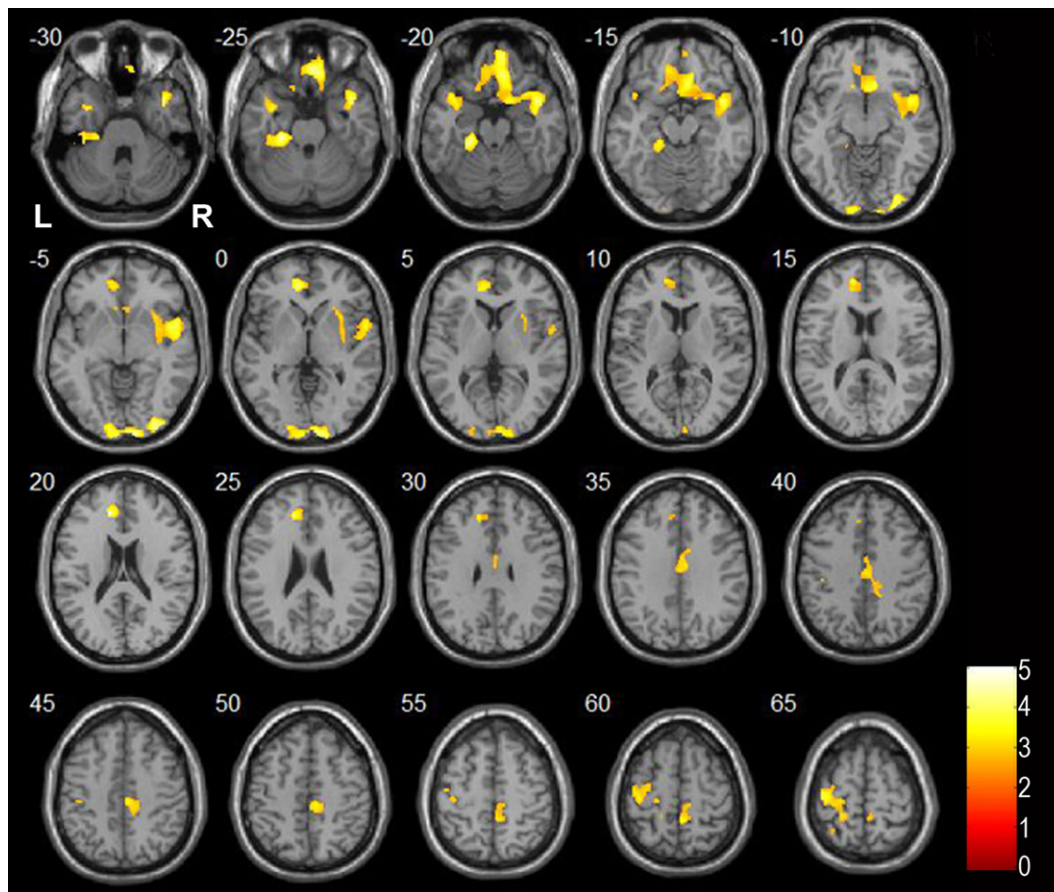


**Fig. 1.** Brain areas in which gray matter volumes (GMVs) show significant correlations ( $P < 0.01$ , corrected) with Raven's Standard Progressive Matrices (RSPM) scores in 297 healthy young adult subjects as revealed by partial correlation analysis controlling for sex and age.

As previously stated, the main function of the salience network is to initiate the CEN and inhibit the DMN, which is consistent with our finding that the RSPM scores were positively correlated with ReHo values in brain areas of the CEN but negatively correlated with those in the DMN. Specifically, the RSPM scores were positively correlated with GMV and ReHo values in the right rostrolateral prefrontal cortex (RLPFC) and the left fusiform and parahippocampal gyri, which are components of the CEN. Activation in the RLPFC has been reported in a wide variety of tasks including attention, working memory and episodic retrieval tasks [51,52]. Moreover, the RLPFC has consistently been implicated in fMRI studies of reasoning tasks [5,8–11,52], is thought to be modulated by relational complexity [8] and is engaged in relational integration and comparison when dealing with relational information associated with

a problem such as RPM [9,11,53]. The correlations between RSPM scores and GMV and ReHo values of the left FG and PHG are not surprising given that these regions are involved in memory processing [54]. Our results are further supported by studies that found that ReHo values [24], GMV [17,20] and cortical thickness [44] in these areas were correlated with IQ scores in healthy adults. In contrast, significant negative associations were found between RSPM scores and ReHo values in the PCC/Pcu and right inferior partial lobule, core nodes of the DMN. The DMN is preferentially activated when an individual focuses on internal tasks such as day-dreaming, retrieving a memory or envisioning the future, and is routinely deactivated in response to cognitively demanding tasks [37,38,55,56]. Our findings support the hypothesis that a superior capacity of fluid reasoning may be related to better development

**Table 3**  
Brain areas whose ReHo values show significant correlations ( $P < 0.01$ , corrected) with RSPM scores.

Brain regions	Brodmann areas	Cluster size (voxels)	Peak <i>t</i> values	Peak coordination in MNI (x, y, z)
<b>Positive correlations</b>				
Right middle frontal gyrus	10/11	380	4.16*	40, 50, -4
Right FIC	47	106	4.08	34, 18, -24
Right anterior temporal lobe	21/38	465	4.05	50, 12, -24
Left FG, PHG and cerebellar lobule VI	20/36/37	163	3.53	-36, -44, -30
<b>Negative correlations</b>				
Right inferior parietal lobule	40	201	-3.87	32, -38, 44
Right sensorimotor cortex	3/4	116	-3.86	10, -24, 50
PCC/Pcu	7/31	491	-3.80	6, -72, 26
Left sensorimotor cortex	4/6	85	-3.50	-30, -14, 46

Abbreviations: FIC, fronto-insular cortex; FG, fusiform gyrus; MNI, Montreal Neurological Institute; PCC/Pcu, posterior cingulate cortex/precuneus; PHG, parahippocampal gyrus; ReHo, regional homogeneity; RSPM, Raven's Standard Progressive Matrices.

\*  $P < 0.01$ , corrected.

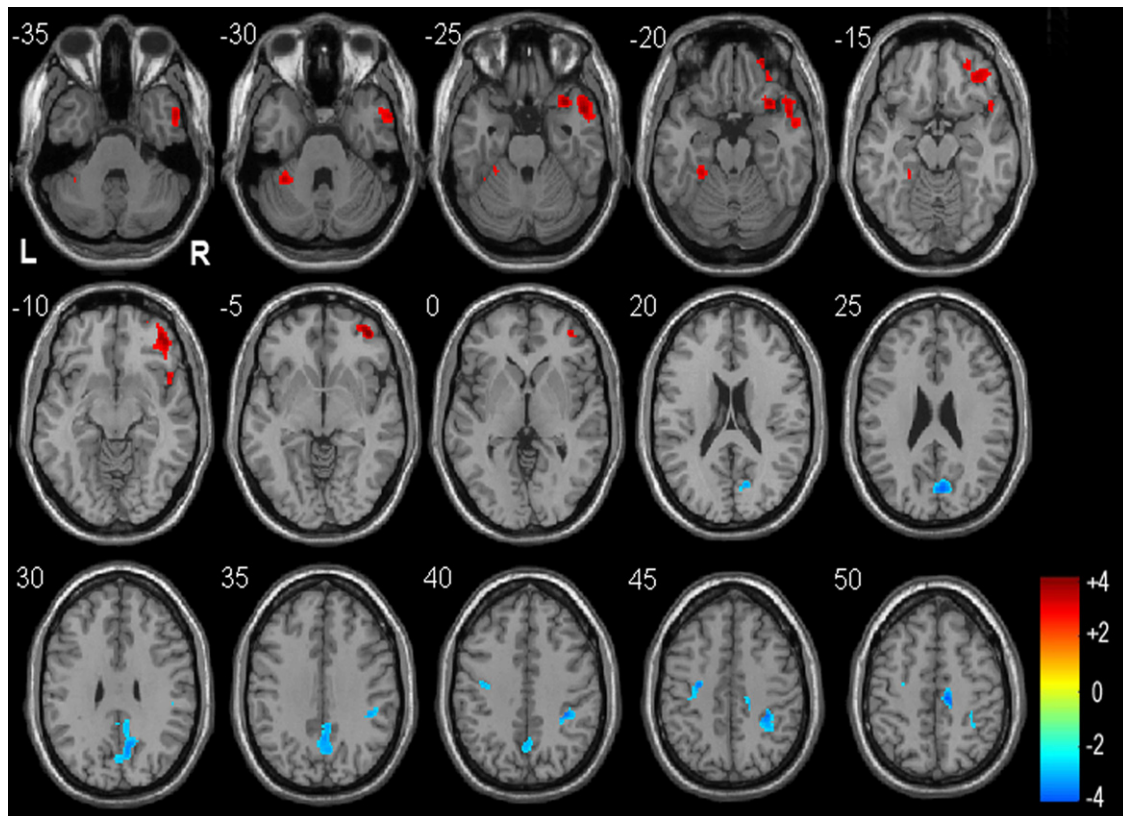


**Fig. 2.** Brain areas in which regional homogeneity (ReHo) values show significant correlations ( $P < 0.01$ , corrected) with Raven's Standard Progressive Matrices (RSPM) scores in 284 subjects as revealed by partial correlation analysis controlling for sex and age. Red denotes positive correlations, and blue denotes negative correlations. (For interpretation of the references to color in this figure legend, the reader is referred to the web version of the article.)

of the salience network and CEN and poorer development of the posterior part of the DMN.

Neuropsychological studies have shown that the OFC is implicated in reasoning. Based on lesion and functional imaging studies, Elliott proposed that the OFC is primarily involved in the processes of making responses, monitoring associations, and making further choices using previous information [57]. A VBM study showed that the GMV of OFC (BA11) was positively correlated with IQ [19]. More recently, a diffusion MRI study demonstrated that the right uncinate fasciculus, a white matter tract connecting the anterior part of the temporal lobe to the orbitofrontal cortex, was the only tract whose integrity was correlated with intelligence in healthy adults [22]. These findings are consistent with our findings of correlations between RSPM scores and GMV and ReHo values in the anterior temporal cortex and OFC in healthy young subjects.

The visual cortex is involved in updating information in working memory by making comparisons among visual images and modulating visual attention. These functions are critically important for dealing with fluid reasoning tasks. Therefore, it is reasonable that a positive correlation was detected between GMVs of the visual cortex and RSPM scores in our study, and this correlation is consistent with the positive correlations found between GMVs and IQ [20,42] and activation of the visual cortex during a variety of cognitive tasks, particularly RPM relational reasoning [3,5,7,45,46]. The results of our study, in addition to those of the studies mentioned above, suggest that the visual cortex may play an important role in the performance of tasks that use non-verbal visuospatial contexts to assess fluid reasoning. This hypothesis is also supported by studies of autistic children who had superior visuospatial ability but inferior semantic performance and showed significantly increased activation [45] and cortical thickness [58] in the visual cortex.

Despite the fact that sensorimotor areas are mainly involved in receiving sensory inputs and planning and executing voluntary motor movements, the GMVs of these areas were positively correlated with IQ [17,19] and visuospatial cognition processing [59], a critical capability for solving reasoning problems. Moreover, the sensorimotor areas were frequently activated during cognitive tasks associated with relational reasoning [12,46,60]. In the parietal–frontal theory of intelligence model (P-FIT), sensorimotor areas are engaged in generating appropriate responses in the final processing of intelligence [47]. Our finding of a positive correlation between RSPM scores and GMVs of these areas is consistent with the findings mentioned above. However, we also found a negative correlation between ReHo values of these areas and RSPM scores. That is to say, individuals with lower RSPM scores had higher ReHo values in the sensorimotor areas (See Fig. S1 in Supplementary Materials), which may reflect functional compensation for the lower capacity of fluid reasoning to maintain normal cognitive function in these subjects. This hypothesis will require further validation.

There are several limitations to this study. An important limitation of this study is that we did not conduct task-based functional MRI on our subjects. As such, we cannot directly verify the role of the salience network on RSPM problem-solving processing. Another limitation is the lack of a control measure that would examine goal-oriented tasks with lower cognitive load. Thus, we cannot exclude the possibility that the salience network would be engaged regardless of the goal-oriented task. We analyzed correlations of anxiety scores as assessed by the Self-Rating Anxiety Scale [61] with GMV and ReHo and found that anxiety scores were not correlated with the GMV or ReHo of the salience network (under the same thresholds used in RSPM analysis; see Figs. S2 and S3 in Supplementary Materials). Therefore, we speculate that the structural

and functional characteristics of the salience network are related to goal-oriented tasks (such as RSPM) but are not inevitably related to other psychometric measures (such as anxiety scores). Further studies are needed to clarify the issue.

In conclusion, we investigated the neural correlates of the capacity of fluid reasoning by combining structural and functional MRI analyses in a large sample of healthy young adults. We found that RSPM scores were correlated with GMVs and ReHo in brain areas of the salient, central executive, default-mode, visual and sensorimotor networks. Our results emphasize the important contribution of the salience network to one's capacity for fluid reasoning.

## Acknowledgements

This work was supported by the Natural Science Foundation of Tianjin (No. 11JCZDJC19300), Natural Science Foundation of China (Nos. 30870694 and 30730036) and the National Basic Research Program of China (973 Program, No. 2010CB732506). The funders had no role in study design, data collection and analysis, interpretation of data, decision to publish, or preparation of the manuscript.

## Appendix A. Supplementary data

Supplementary data associated with this article can be found, in the online version, at doi:10.1016/j.bbr.2012.01.037.

## References

- [1] Perfetti B, Saggino A, Ferretti A, Caulo M, Romani GL, Onofri M. Differential patterns of cortical activation as a function of fluid reasoning complexity. *Hum Brain Mapp* 2009;30:497–510.
- [2] Gray JR, Thompson PM. Neurobiology of intelligence: science and ethics. *Nat Rev Neurosci* 2004;5:471–82.
- [3] Kalbfleisch ML, Van Meter JW, Zeffiro TA. The influences of task difficulty and response correctness on neural systems supporting fluid reasoning. *Cogn Neurodyn* 2007;1:71–84.
- [4] Snow RE, Kyllonen PC, Marshalek B. The topography of ability and learning correlations. In: Sternberg R, editor. *Advances in the psychology of human intelligence*, vol. 2. Hillsdale, NJ: Erlbaum; 1984. p. 47–103.
- [5] Prabhakaran V, Smith JA, Desmond JE, Glover GH, Gabrieli JD. Neural substrates of fluid reasoning: an fMRI study of neocortical activation during performance of the Raven's Progressive Matrices Test. *Cogn Psychol* 1997;33:43–63.
- [6] Duncan J, Seitz RJ, Kolodny J, Bor D, Herzog H, Ahmed A, et al. A neural basis for fluid intelligence. *Science* 2000;289:457–60.
- [7] Goel V, Dolan RJ. Functional neuroanatomy of three-term relational reasoning. *Neuropsychologia* 2001;39:901–9.
- [8] Wright SB, Matlen BJ, Baym CL, Ferrer E, Bunge SA. Neural correlates of fluid reasoning in children and adults. *Front Hum Neurosci* 2007;1:8.
- [9] Christoff K, Prabhakaran V, Dorfman J, Zhao Z, Kroger JK, Holyoak KJ, et al. Rostrolateral prefrontal cortex involvement in relational integration during reasoning. *Neuroimage* 2001;14:1136–49.
- [10] Kroger JK, Sabb FW, Fales CL, Bookheimer SY, Cohen MS, Holyoak KJ. Recruitment of anterior dorsolateral prefrontal cortex in human reasoning: a parametric study of relational complexity. *Cereb Cortex* 2002;12:477–85.
- [11] Wendelken C, Nakhachenko D, Donohue SE, Carter CS, Bunge SA. "Brain is to thought as stomach is to food": investigating the role of rostral prefrontal cortex in relational reasoning. *J Cogn Neurosci* 2008;20:682–93.
- [12] Goel V, Dolan RJ. Differential involvement of left prefrontal cortex in inductive and deductive reasoning. *Cognition* 2004;93:B109–21.
- [13] Esposito G, Kirkby BS, Van Horn JD, Ellmore TM, Berman KF. Context-dependent, neural system-specific neurophysiological concomitants of ageing: mapping PET correlates during cognitive activation. *Brain* 1999;122(Pt 5):963–79.
- [14] Gray JR, Chabris CF, Braver TS. Neural mechanisms of general fluid intelligence. *Nat Neurosci* 2003;6:316–22.
- [15] Lee KH, Choi YY, Gray JR, Cho SH, Chae JH, Lee S, et al. Neural correlates of superior intelligence: stronger recruitment of posterior parietal cortex. *Neuroimage* 2006;29:578–86.
- [16] Deary IJ, Penke L, Johnson W. The neuroscience of human intelligence differences. *Nat Rev Neurosci* 2010;11:201–11.
- [17] Haier RJ, Jung RE, Yeo RA, Head K, Alkire MT. Structural brain variation and general intelligence. *Neuroimage* 2004;23:425–33.
- [18] Wilke M, Sohn JH, Byars AW, Holland SK. Bright spots: correlations of gray matter volume with IQ in a normal pediatric population. *Neuroimage* 2003;20:202–15.
- [19] Frangou S, Chitnis X, Williams SC. Mapping IQ and gray matter density in healthy young people. *Neuroimage* 2004;23:800–5.
- [20] Haier RJ, Jung RE, Yeo RA, Head K, Alkire MT. The neuroanatomy of general intelligence: sex matters. *Neuroimage* 2005;25:320–7.
- [21] Luders E, Narr KL, Thompson PM, Toga AW. Neuroanatomical correlates of intelligence. *Intelligence* 2009;37:156–63.
- [22] Yu C, Li J, Liu Y, Qin W, Li Y, Shu N, et al. White matter tract integrity and intelligence in patients with mental retardation and healthy adults. *Neuroimage* 2008;40:1533–41.
- [23] Chiang MC, Barysheva M, Shattuck DW, Lee AD, Madsen SK, Avedissian C, et al. Genetics of brain fiber architecture and intellectual performance. *J Neurosci* 2009;29:2212–24.
- [24] Li Y, Liu Y, Li J, Qin W, Li K, Yu C, et al. Brain anatomical network and intelligence. *PLoS Comput Biol* 2009;5:e1000395.
- [25] Wang L, Song M, Jiang T, Zhang Y, Yu C. Regional homogeneity of the resting-state brain activity correlates with individual intelligence. *Neurosci Lett* 2011;488:275–8.
- [26] Song M, Zhou Y, Li J, Liu Y, Tian L, Yu C, et al. Brain spontaneous functional connectivity and intelligence. *Neuroimage* 2008;41:1168–76.
- [27] van den Heuvel MP, Stam CJ, Kahn RS, Hulshoff Pol HE. Efficiency of functional brain networks and intellectual performance. *J Neurosci* 2009;29:7619–24.
- [28] Gong Q-Y, Sluming V, Mayes A, Keller S, Barrick T, Cezayirli E, et al. Voxel-based morphometry and stereology provide convergent evidence of the importance of medial prefrontal cortex for fluid intelligence in healthy adults. *Neuroimage* 2005;25:1175–86.
- [29] Yoshiura T, Hiwatashi A, Yamashita K, Ohyagi Y, Monji A, Takayama Y, et al. Deterioration of abstract reasoning ability in mild cognitive impairment and Alzheimer's disease: correlation with regional grey matter volume loss revealed by diffeomorphic anatomical registration through exponentiated lie algebra analysis. *Eur Radiol* 2011;21:419–25.
- [30] Baldo JV, Bunge SA, Wilson SM, Dronkers NF. Is relational reasoning dependent on language? A voxel-based lesion symptom mapping study. *Brain Lang* 2010;113:59–64.
- [31] Carpenter PA, Just MA, Shell P. What one intelligence test measures: a theoretical account of the processing in the Raven Progressive Matrices Test. *Psychol Rev* 1990;97:404–31.
- [32] Raven JC. *Standard progressive matrices: sets A, B, C, D and E*. Oxford: Oxford Psychologists Press; 1976.
- [33] Ashburner J. A fast diffeomorphic image registration algorithm. *Neuroimage* 2007;38:95–113.
- [34] Zang Y, Jiang T, Lu Y, He Y, Tian L. Regional homogeneity approach to fMRI data analysis. *Neuroimage* 2004;22:394–400.
- [35] Seeley WW, Menon V, Schatzberg AF, Keller J, Glover GH, Kenna H, et al. Dissociable intrinsic connectivity networks for salience processing and executive control. *J Neurosci* 2007;27:2349–56.
- [36] Sridharan D, Levitin DJ, Menon V. A critical role for the right fronto-insular cortex in switching between central-executive and default-mode networks. *Proc Natl Acad Sci USA* 2008;105:12569–74.
- [37] Fox MD, Snyder AZ, Vincent JL, Corbetta M, Van Essen DC, Raichle ME. The human brain is intrinsically organized into dynamic, anticorrelated functional networks. *Proc Natl Acad Sci USA* 2005;102:9673–8.
- [38] Greicius MD, Krasnow B, Reiss AL, Menon V. Functional connectivity in the resting brain: a network analysis of the default mode hypothesis. *Proc Natl Acad Sci USA* 2003;100:253–8.
- [39] Menon V, Uddin LQ. Saliency, switching, attention and control: a network model of insula function. *Brain Struct Funct* 2010;214:655–67.
- [40] Nimchinsky EA, Gilissen E, Allman JM, Perl DP, Erwin JM, Hof PR. A neuronal morphologic type unique to humans and great apes. *Proc Natl Acad Sci USA* 1999;96:5268–73.
- [41] Allman JM, Watson KK, Tetreault NA, Hakeem AY. Intuition and autism: a possible role for Von Economo neurons. *Trends Cogn Sci* 2005;9:367–73.
- [42] Colom R, Jung RE, Haier RJ. Distributed brain sites for the g-factor of intelligence. *Neuroimage* 2006;31:1359–65.
- [43] Pennington BF, Filipek PA, Lefty D, Chhabildas N, Kennedy DN, Simon JH, et al. A twin MRI study of size variations in human brain. *J Cogn Neurosci* 2000;12:223–32.
- [44] Narr KL, Woods RP, Thompson PM, Szeszko P, Robinson D, Dimtcheva T, et al. Relationships between IQ and regional cortical gray matter thickness in healthy adults. *Cereb Cortex* 2007;17:2163–71.
- [45] Soulières I, Dawson M, Samson F, Barbeau EB, Sahyoun CP, Strangman GE, et al. Enhanced visual processing contributes to matrix reasoning in autism. *Hum Brain Mapp* 2009;30:4082–107.
- [46] Dumontheil I, Houlton R, Christoff K, Blakemore SJ. Development of relational reasoning during adolescence. *Dev Sci* 2010;13:F15–24.
- [47] Jung RE, Haier RJ. The parieto-frontal integration theory (P-FIT) of intelligence: converging neuroimaging evidence. *Behav Brain Sci* 2007;30:135–54 [discussion 54–87].
- [48] Seeley WW. Anterior insula degeneration in frontotemporal dementia. *Brain Struct Funct* 2010;214:465–75.
- [49] Zhou J, Greicius MD, Gennatas ED, Growdon ME, Jang JY, Rabinovici GD, et al. Divergent network connectivity changes in behavioural variant frontotemporal dementia and Alzheimer's disease. *Brain* 2010;133:1352–67.
- [50] Habas C, Kamdar N, Nguyen D, Prater K, Beckmann CF, Menon V, et al. Distinct cerebellar contributions to intrinsic connectivity networks. *J Neurosci* 2009;29:8586–94.
- [51] Gilbert SJ, Spengler S, Simons JS, Steele JD, Lawrie SM, Frith CD, et al. Functional specialization within rostral prefrontal cortex (area 10): a meta-analysis. *J Cogn Neurosci* 2006;18:932–48.

- [52] Bunge SA, Helskog EH, Wendelken C. Left, but not right, rostrolateral prefrontal cortex meets a stringent test of the relational integration hypothesis. *Neuroimage* 2009;46:338–42.
- [53] Crone EA, Wendelken C, van Leijenhorst L, Honomichl RD, Christoff K, Bunge SA. Neurocognitive development of relational reasoning. *Dev Sci* 2009;12:55–66.
- [54] Binder JR, Desai RH, Graves WW, Conant LL. Where is the semantic system? A critical review and meta-analysis of 120 functional neuroimaging studies. *Cereb cortex* 2009;19:2767–96.
- [55] Raichle ME, MacLeod AM, Snyder AZ, Powers WJ, Gusnard DA, Shulman GL. A default mode of brain function. *Proc Natl Acad Sci USA* 2001;98:676–82.
- [56] Fox MD, Raichle ME. Spontaneous fluctuations in brain activity observed with functional magnetic resonance imaging. *Nat Rev Neurosci* 2007;8:700–11.
- [57] Elliott R, Dolan RJ, Frith CD. Dissociable functions in the medial and lateral orbitofrontal cortex: evidence from human neuroimaging studies. *Cereb Cortex* 2000;10:308–17.
- [58] Hyde KL, Samson F, Evans AC, Mottron L. Neuroanatomical differences in brain areas implicated in perceptual and other core features of autism revealed by cortical thickness analysis and voxel-based morphometry. *Hum Brain Mapp* 2010;31:556–66.
- [59] Hanggi J, Buchmann A, Mondadori CR, Henke K, Jancke L, Hock C. Sexual dimorphism in the parietal substrate associated with visuospatial cognition independent of general intelligence. *J Cogn Neurosci* 2010;22:139–55.
- [60] Golde M, von Cramon DY, Schubotz RI. Differential role of anterior prefrontal and premotor cortex in the processing of relational information. *Neuroimage* 2010;49:2890–900.
- [61] Zung WW. A rating instrument for anxiety disorders. *Psychosomatics* 1971;12:371–9.